

SPATIAL AND SEASONAL VARIABILITY IN THE DIURNAL CYCLE OF WARM-SEASON PRECIPITATION

Phillip A. Arkin¹, Pingping Xie², Robert Joyce³,
and John Janowiak⁴,

1. INTRODUCTION

Precipitation, particularly in the tropics and during the warm season in midlatitudes, exhibits strong variability over the diurnal cycle. Observational studies using relatively coarse observational datasets based on surface observations as well as satellite data have shown that this variability has substantial spatial and seasonal variability that is poorly simulated by state-of-the-art atmospheric models (Meisner and Arkin, 1987; Dai and Trenberth, 2001). However, the fine details of these variations have been impossible to observe in most parts of the world until now. CMORPH (Joyce et al., 2004) is a very high resolution (~ 8 km in space, 30 minutes in time) analysis of precipitation for the globe ($60^{\circ}\text{N} - 60^{\circ}\text{S}$) that is derived by combining precipitation estimates from passive microwave radiometers with storm motion inferred from geostationary infrared data. Its high resolution enables us to describe precipitation variability over many areas with unprecedented detail, comparable to that made possible by national radar networks or enhanced observing systems characteristic of transient field programs.

In this paper, we use CMORPH-derived precipitation averaged over 3 hourly periods and areas of 0.25° latitude/longitude to describe the seasonal and interannual variations in the diurnal cycle during the Northern Hemisphere warm seasons of 2003 and 2004 over North America and the nearby oceans. Areas of emphasis include: land-sea contrast in the diurnal cycle, the effect of orography, and the relationship of interannual variability in circulation and total precipitation to changes in the diurnal cycle. Where appropriate, we will supplement our results with comparisons between precipitation derived from operational NWS radar observations

¹ESSIC, University of Maryland, College Park

² NOAA, Climate Prediction Center, Camp Springs

³ NOAA, Climate Prediction Center, Camp Springs

⁴ NOAA, Climate Prediction Center, Camp Springs

and geostationary satellite observations of cold cloud.

2. SEASONAL MEAN PRECIPITATION

Figure 1 shows the mean precipitation for the May – September 2003 period, in mm/day, for North America and nearby oceanic regions. The principal features are similar to those found in previous studies of summer precipitation: a pronounced maximum in the Intertropical Convergence Zone (ITCZ), between $5^{\circ}\text{--}10^{\circ}\text{N}$, with smaller maxima over the Sierra Madre Occidental (SMO) Mountains of western Mexico, the Southeast US, and off the Southeast US coast. The right hand panel of figure 1 shows the terrain elevation over the region, allowing us to see more clearly the relationship between the SMO and the precipitation maximum. Note also the minimum in precipitation that separates the maximum over the SMO from the ITCZ – since CMORPH is based originally on estimates from passive microwave observations, and since all algorithms for computing such estimates are prone to difficulties in coastal regions (Arkin and Ardanuy, 1989), we cannot be sure of the reality of this minimum without corroborating evidence.

3. MEAN DIURNAL CYCLE

We will examine the mean diurnal cycle during the period May – September 2003 using precipitation derived from CMORPH and averaged over 3 hour periods (0000–0230 UTC, 0300–0530 UTC, and so on) for selected regions. In figure 2, we show the mean diurnal cycle relative to the peak elevation of the SMO for the period. (Note: in all the plots of mean diurnal cycle, the averages for a given 3-hour period are plotted at the time of the beginning of that period.) Following a diurnal minimum in precipitation of < 1 mm/day at about 8 am (1500 UTC – local solar time at this longitude is about UTC – 0700), an increase is seen very near at the peak elevation. Values > 8 mm/day are found by local noon, and persist through the daylight hours and into the night. The longitude of maximum precipitation shows some progression westward, but to a very limited degree. Precipitation west of the Gulf of California remains below 4 mm/day, and with only a minimal diurnal cycle apparent over the Pacific Ocean. These results reveal a diurnal cycle that is very coherent throughout the season, and one that is strongly tied to the highest terrain.

Figure 3 shows the mean diurnal cycle of precipitation averaged between $90^{\circ}\text{--}115^{\circ}\text{W}$ between the equator and 30°N . This figure shows the transition between precipitation associated with the ITCZ, which exhibits a strong

maximum with a weak diurnal cycle, peaking during the nighttime, and that associated with the elevated terrain in southern Mexico, which has a pronounced diurnal minimum in the early morning and a maximum in late afternoon. The southern coast of Mexico, near 15°N, coincides with a pronounced minimum in total precipitation, and a discontinuity in the character of diurnal variability.

Figure 4 shows the diurnal cycle in precipitation from CMORPH averaged over the May – September 2003 period between 35°–40°N along an east-west transect from 110°–60°W. This area extends from just west of the peak elevation of the Rocky Mountains to a point well east of the US coastline. A pronounced diurnal cycle is seen to be associated with the highest terrain in the west, with a minimum in the early morning hours and a maximum shortly after local noon (local solar time is UTC – 0700 at 105°W). A somewhat similar cycle is seen at about 80°W associated with the elevated terrain in the eastern US.

This figure contains two other noteworthy features: the evident eastward propagation of the diurnal peak from 105°W for at least 12 hours, and possibly longer, and the strong diurnal cycle with a nighttime maximum associated with the maximum in precipitation off the US East Coast. The first of these is consistent with the results of Carbone et al. (2002) from analyses of radar rainfall over the US. The second can be seen in the radar data as well (not shown), but only further south, where this feature is within range of the operational coastal radar network.

4. SUMMARY AND FURTHER WORK

Thus far, this project has demonstrated the potential of CMORPH to elucidate the subtle features of diurnal precipitation variability associated with mountains and coastlines in particular. We plan to extend this analysis to the year 2004 and to the monthly time scale, which will enable us to begin to examine the degree to which the identified phenomena vary interannually and intraseasonally. Over the US, we will also utilize radar-derived estimates of rainfall as well as analyses based on gauge observations to determine the uncertainties in the CMORPH-derived estimates of diurnal variability.

5. REFERENCES

- Arkin, P.A., and P.E. Ardanuy, 1989: Estimating Climatic-Scale Precipitation from Space: A Review. *J. Climate*, **2**, 1229–1238.
- Carbone, R.E., J.D. Tuttle, D.A. Ahijevych, and S.B. Trier, 2002: Inferences of Predictability Associated with Warm Season Precipitation Episodes. *J. Atmos. Sci.*, **59**, 2033–2056.
- Dai, A., and K.E. Trenberth, 2004: The Diurnal Cycle and Its Depiction in the Community Climate System Model. *J. Climate*, **17**, 930–951.
- Joyce, R.J., J.E. Janowiak, P.A. Arkin, and P. Xie, 2004: CMORPH: A Method that Produces Global Precipitation Estimates from Passive Microwave and Infrared Data at High Spatial and Temporal Resolution. *J. Hydrometeorology*, **5**, 487–503.
- Meisner, B.N., and P.A. Arkin, 1987: Spatial and Annual Variations in the Diurnal Cycle of Large-Scale Tropical Convective Cloudiness and Precipitation. *Mon. Wea. Rev.*, **115**, 2009–2032.

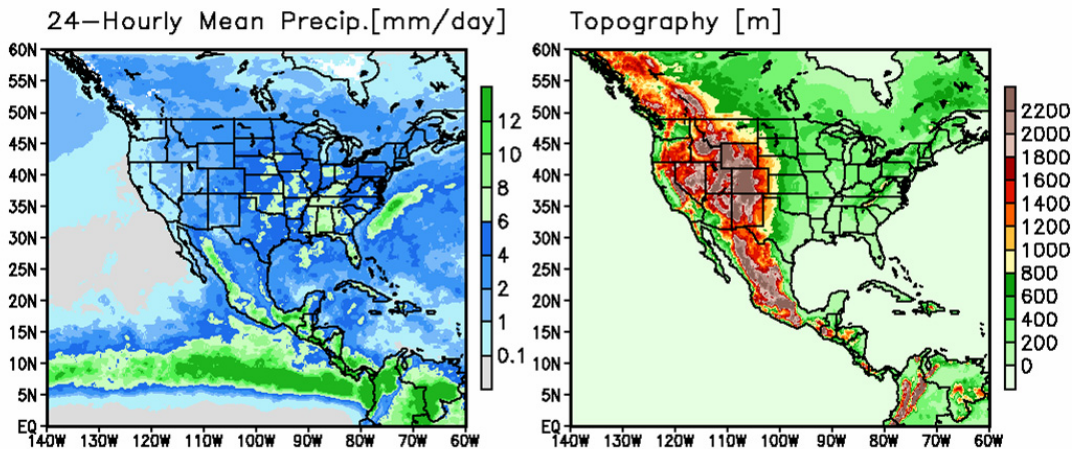


Figure 1. Mean daily precipitation from CMORPH for May – September 2003 (left) and surface elevation (right).

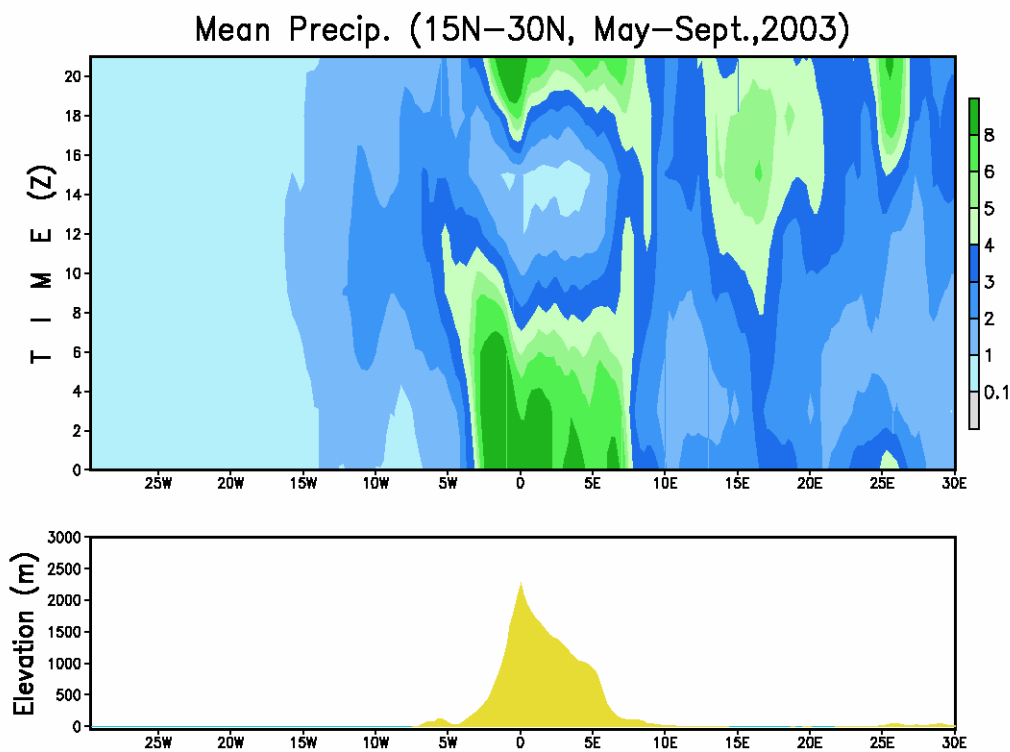


Figure 2. Mean diurnal cycle of precipitation (May – September 2003) averaged over 15°–30°N relative to longitude of highest elevation (top) and mean elevation over the same region (bottom).

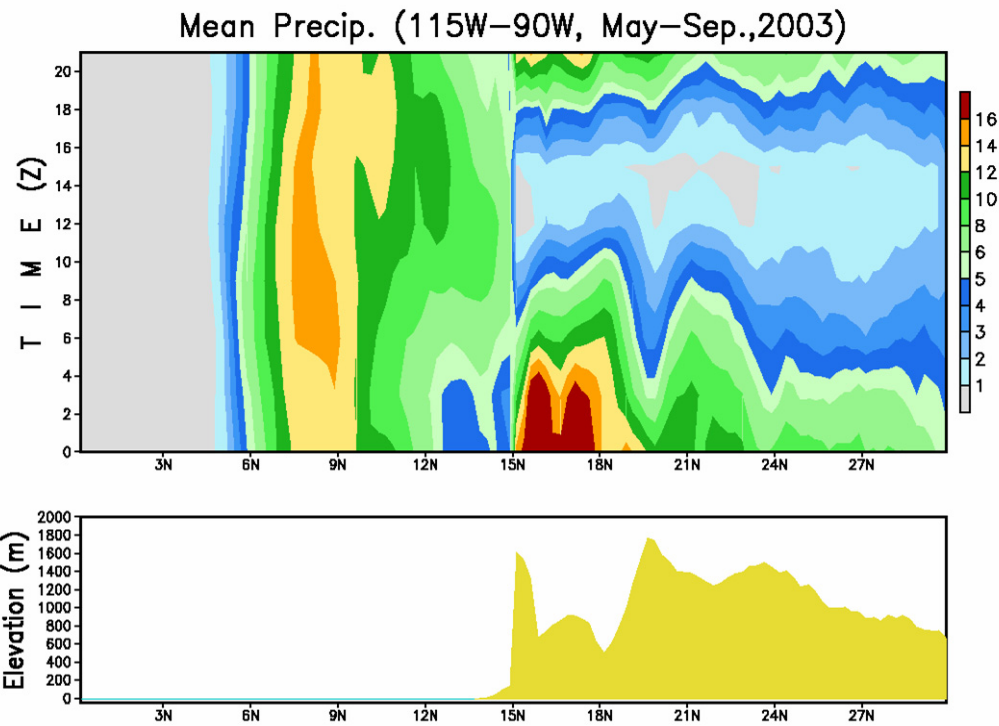


Figure 3. As in figure 2 except averaged between 90° - 115° W along a north-south transect from the equator to 30° N. The lower panel shows terrain elevation averaged similarly.

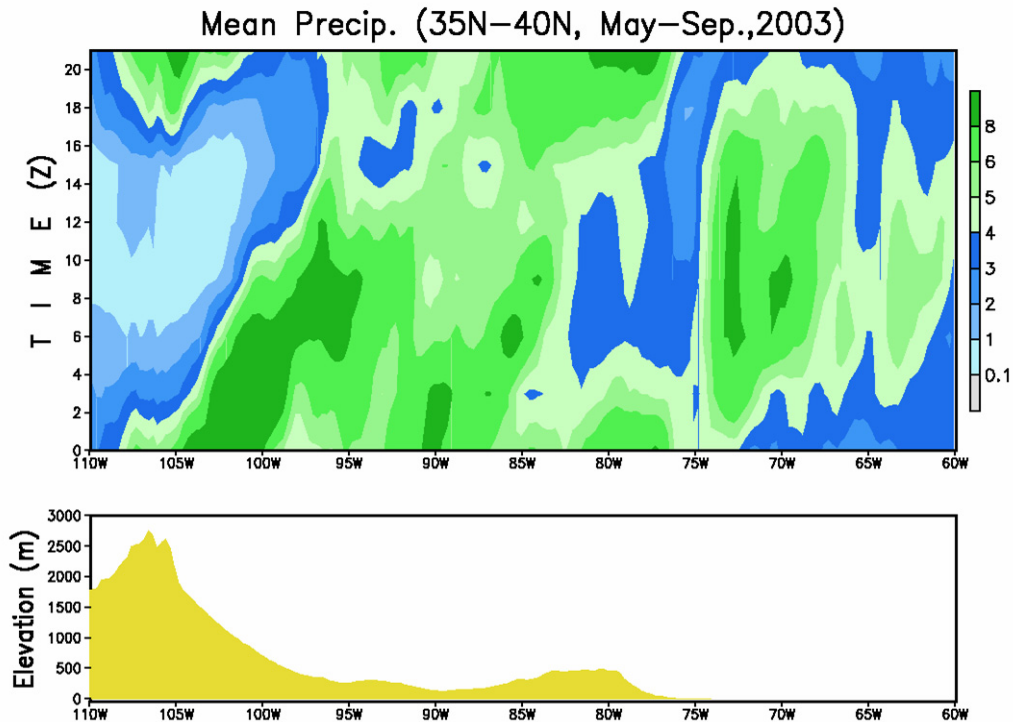


Figure 4. As in figure 2 except averaged between 35° - 40° N along an east-west transect from 60° - 110° W. The lower panel shows terrain elevation averaged similarly.